



# Effect of silicon anisotropy on the stability of thermomigration of linear zones

Boris M. Seredin<sup>1</sup> · Victor P. Popov<sup>1</sup> · Alexander V. Malibashev<sup>1</sup> · Igor V. Gavrus<sup>1</sup> · Sergey M. Loganchuk<sup>1</sup> · Sergey Y. Martyushov<sup>2</sup>

Received: 1 December 2023 / Accepted: 15 February 2024 / Published online: 7 March 2024  
© The Author(s), under exclusive licence to Springer Nature B.V. 2024

## Abstract

New types of instabilities associated with crystal anisotropy during thermomigration of rectilinear and curvilinear (annular) zones under the action of a temperature gradient in the silicon-aluminium system are experimentally revealed. A force model of thermomigration is improved, which takes into account vectors of resistance forces to atomic-kinetic processes at the dissolution front. This model explains the observed features of the stable and unstable motion of the linear zones. Reasons and a mechanism of thickenings and kinks of the ends of rectilinear zones, their fragmentation and decay, as well as transformation of annular linear zones into triangular and square zones during thermomigration in the  $\langle 111 \rangle$  and  $\langle 100 \rangle$  directions, respectively, were also explained.

**Keywords** Thermomigration · Temperature gradient · Silicon · Crystal anisotropy · Stability

## 1 Background

Liquid inclusions (zones) in solids migrate under the action of a temperature gradient [1]. This phenomenon, known as thermomigration or zone recrystallization with a temperature gradient, is used in physical and chemical studies and as a method for creating electrically heterogeneous structures in electronic equipment [2]. This method is unique because it allows the doping of crystal microregions at a rate from 3 to 4 orders of magnitude higher than a solid-state diffusion [3].

Particular interest is the migration of liquid inclusions that are extended in one dimension; these inclusions are called linear (rectilinear or curvilinear) zones. For example, aluminum-based zones can be used to form epitaxial channels and closed cells of a specific geometry in a silicon wafer, which is useful for power semiconductor devices [4–8]. Electrophysical properties of such channels have been

studied and the high crystal perfection of the obtained structures were confirmed [9, 10].

The widespread application of the thermomigration method is limited by lack of knowledge about the conditions for the stable motion of liquid zones while preserving their shape and a trajectory of motion, specified by temperature gradient. The instability of zone migration leads to a violation of the formed structure's topology and the impossibility of carrying out subsequent operations for device manufacturing.

Analysis of the thermomigration process in isotropic crystal [11] based on the dynamic stability of the crystal-melt interface [12] showed the resilience of the crystallizing "cold" zone boundary to distortions of any shape. On the contrary, the dissolving "hot" boundary is generally dynamically unstable, which leads to distortion of the shape and decay of the zone. These theoretical conclusions were confirmed experimentally [13, 14]. At the same time, surface tension stabilizes the shape of the zone, and the anisotropic atomic kinetics of dissolution can be both stabilizing and destabilizing factors. Therefore, the correct choice of the crystal orientation, the zone, and the temperature gradient makes it possible to stabilize the thermal migration.

The faceting of the liquid zone dissolution front with densely-packed planes  $\{111\}$  and the absence of the crystallization front faceting during thermomigration in silicon

✉ Boris M. Seredin  
seredinboris@gmail.com

<sup>1</sup> Department of Physics and Photonics, Platov South-Russian State Polytechnic University (NPI), Novochebassk, Russian Federation

<sup>2</sup> Technological Institute for Superhard and Novel Carbon Materials, Troitsk, Moscow, Russian Federation

have been experimentally established [15–17]. The rectilinear zone orientation stability rule was formulated, which is reduced to the requirement of symmetrical faceting of the dissolution front with respect to the zone axis and the temperature gradient. According to this rule, for silicon wafers oriented along the planes of {100} or {110}, it is necessary to place the rectilinear zones axes on the surface in the  $\langle 110 \rangle$  directions, and the temperature gradient, as usual, should be directed normally to the wafer. In this case, the dissolution front is limited by two planes of {111}, symmetrical with respect to the zone axis, with an angle  $\alpha$  between the planes  $70^\circ$  and  $110^\circ$  for wafers {100} and {110}, respectively (hereinafter angle values are rounded to a degree). The cross-sectional shapes of the linear zone and the channel to be formed are shown in Fig. 1a.

For {100} wafers, there are two mutually perpendicular  $\langle 110 \rangle$  directions on the surface, satisfying the conditions for stable migration of rectilinear zones. On {110} wafers, there is only one zone-favorable  $\langle 110 \rangle$  direction. When the zone axis deviates from the  $\langle 110 \rangle$  direction, the straightness and integrity of the zone are violated on the surface of {100} and {110} wafers during thermomigration: the shape of the zone becomes fragmented (in the form of rectangles) in the plane of the wafer. Photos of such zones, migrating stably and unstably, are given in [15, 16]. In [17] for silicon wafers {111} a conclusion about stable migration for rectilinear zones of any orientation was made.

An attempt to consider the effect of anisotropy on the rate of thermomigration was made in [2, 18]. According to the force model of thermomigration, the velocity  $v$  of the liquid zone motion is determined by three self-consistent processes: dissolution, crystallization at opposite boundaries of the zone and diffusion transfer of atoms through the zone and can be described by a simple formula:  $v = F / (R_d + R_c + R_t)$ . Here,  $F$  is the driving force of thermomigration caused by the temperature gradient, and  $R_d$ ,  $R_c$ ,  $R_t$  – resistance to the processes of dissolution, crystallization and transfer of atoms respectively. The expressions for  $F$  and various  $R_d$ ,  $R_c$ ,  $R_t$  are determined through the parameters of thermomigration and the phase diagram of the used system components [18]. For example, for a normal atomic dissolution mechanism:

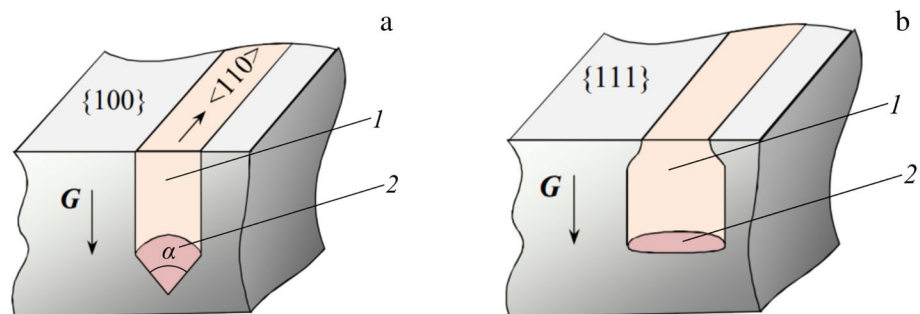
$R_d = RTm / ((c_s - c_L)lv_d)$ , where  $R$  – universal gas constant,  $T$  – absolute temperature,  $m = dc_L/dT$ ,  $c_s$  and  $c_L$  is the concentration of silicon in the solid and liquid phases respectively,  $l$  is the thickness of the zone in the direction of movement. The effect of anisotropy on the migration rate is formally taken into account by the introduction of atomic kinetic coefficients  $v_d$ ,  $v_c$  in expressions and for three known mechanisms: normal, dislocation or two-dimensional nucleation. However, this approach does not explain the instability of thermomigration associated with a possible deviation of the trajectory of the zone from the temperature gradient, described, for example, in [19].

The purpose of this work is to study the stability of thermomigration of rectilinear zones and curvilinear (annular) zones, to explain the observed features of the movement of zones associated with silicon anisotropy.

## 2 Experiment

To obtain the zones, on the starting surface of the silicon wafer a layer of aluminum with thickness 10–15  $\mu\text{m}$  was deposited by magnetron sputtering. Then, using photolithography, a system of parallel rectilinear or curvilinear zones in the form of rings was created. The length of rectilinear zones is 20–90 mm and a diameter of curvilinear zones is 2–5 mm. The aluminum strips for the zones had a width of 100–200  $\mu\text{m}$ . The thermomigration was carried out in a vacuum water-cooled chamber at temperatures of 1300–1600 K. The heating device made it possible to adjust and keep uniform the temperature gradient in the silicon wafer from 20 to 100 K/cm. The tangential component of the temperature gradient did not exceed 1 K/cm. The experiments were carried out on monocrystalline silicon wafers with orientations {111} and {100}, n-type conductivity, resistivity 4.5  $\Omega\cdot\text{cm}$ , dislocation density  $10^2 \text{ cm}^{-2}$ , diameter 100 mm, thickness 0.5–2.0 mm. The nature of the zones' motion was studied by metallographic analysis according to the shapes of epitaxial channels and zones on the polished sections parallel and perpendicular to the surface of the plates.

**Fig. 1** Cross-section diagrams of linear zones and channels obtained on silicon wafers with crystal orientation {100} (a) and {111} (b) Zone axis has the direction  $\langle 110 \rangle$  (a) and any direction, except  $\langle 110 \rangle$  (b). 1 – channel, 2 – zone,  $G$  – temperature gradient



### 3 Rectilinear zones

Experiments revealed new types of instabilities associated with the anisotropy of a crystal under migration in the  $\langle 111 \rangle$  direction. On the wafers  $\{111\}$  for rectilinear

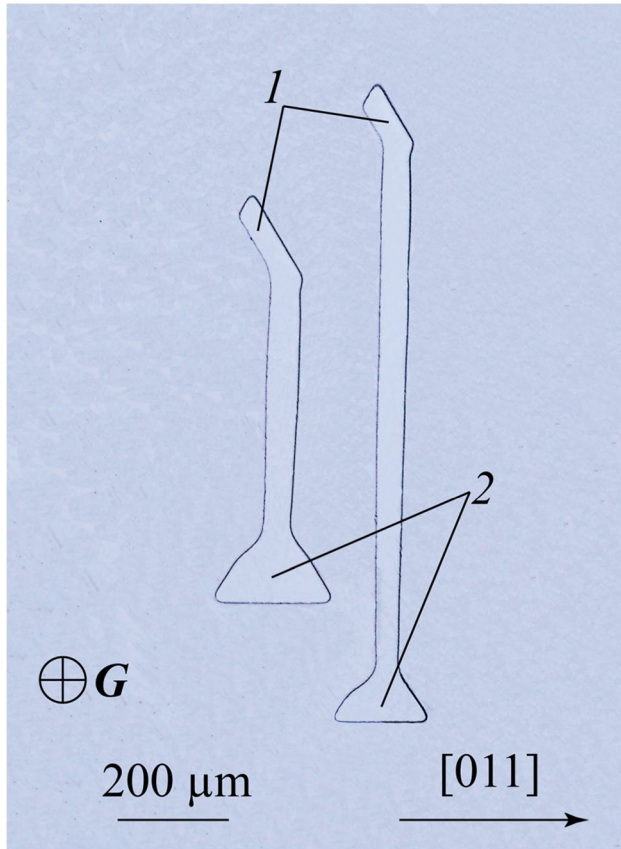
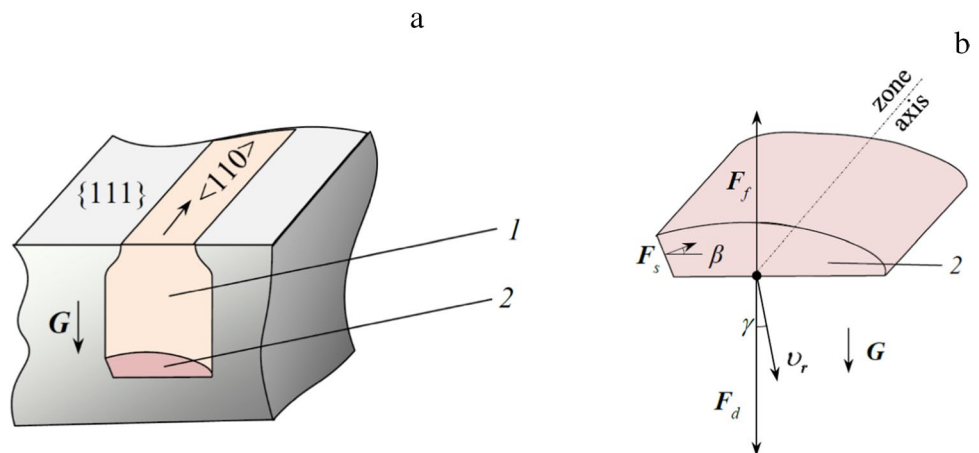


**Fig. 2** Photo of epitaxial channels in the plane of the silicon wafer  $\{111\}$  from the exit side of the originally rectilinear zones. Peculiar kinks (1) and thickenings (2) at the ends of channels. The thickness of the wafer is 0.8 mm

**Fig. 3** Cross-sectional diagrams of rectilinear zone and channel formed on the silicon wafer  $\{111\}$  when the zone axis is oriented along direction  $\langle 110 \rangle$  (a) and the forces acting on the dissolution front of the zone in this case (b). 1 – channel, 2 – zone,  $G$  – temperature gradient



zones oriented within about  $\sim 20^\circ$  in both directions from the normal to the direction  $\langle 110 \rangle$ , thickenings at the ends of the zone and the formed epitaxial channel are observed (Fig. 2). At angles more than  $\sim 20^\circ$  instead of thickening at the ends of rectilinear zones, the kinks of the zones and channel were revealed in the plane of the wafer (see Fig. 2). Kink begin at the ends of the zone. Direction of kinked section matches with direction  $\langle 110 \rangle$ . The length of the kinked section of the zone increases during the migration process. The angle between the initial direction of the zone and the kinked section is kept constant. The epitaxial channel formed by kinked section deviates from the normal to the wafer.

During the migration of rectilinear zones oriented in the direction  $\langle 110 \rangle$  on silicon wafers  $\{100\}$ , the thickenings are also emerged but there were no kinks at the end of the zones.

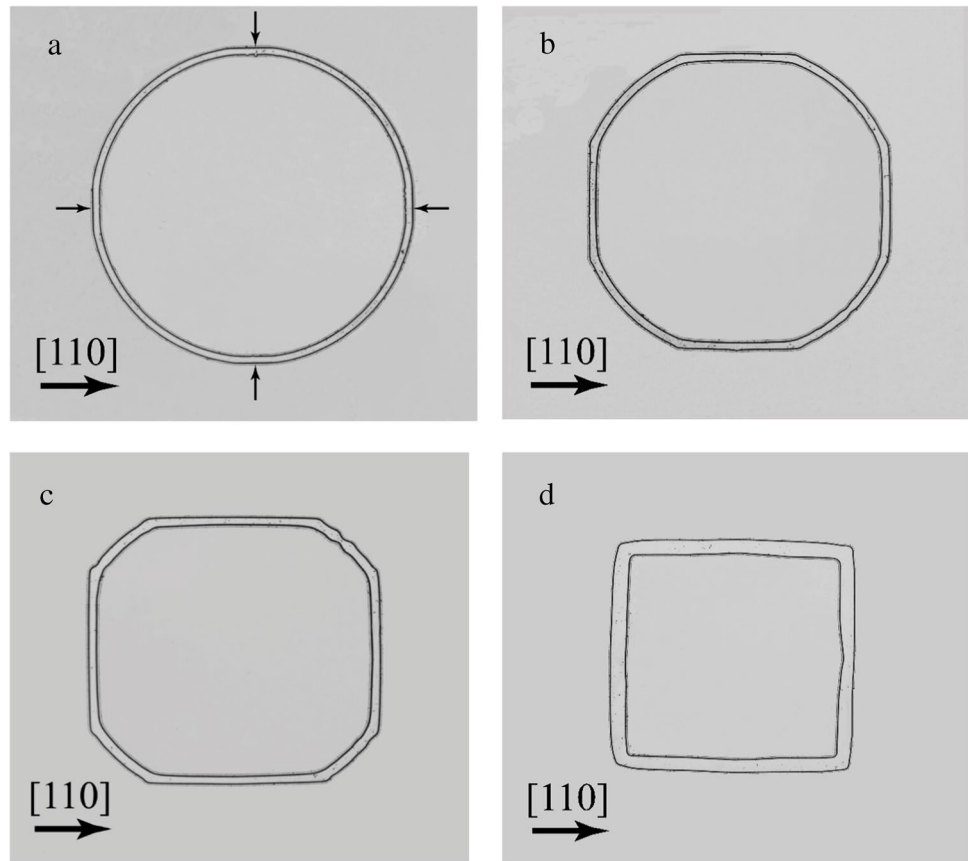
In addition, it was found that the dissolution front of the liquid zone during the migration in the  $\langle 111 \rangle$  direction is faceted in different ways, depending on the orientation of the rectilinear zone. For the zone coinciding with the  $\langle 110 \rangle$  direction, the dissolution front is faceted by two  $\{111\}$  planes: frontal and lateral, located at an angle of  $110^\circ$  and parallel to the zone axis (Fig. 3). For any other orientations of rectilinear zones on the wafer, there is only one frontal plane  $\{111\}$  of the facet on the dissolution front (Fig. 1b).

It corresponds with known observations [17]. This feature of rectilinear zones cross-section is a reason (as shown below) for instability at the ends of rectilinear zones and deviation of trajectory of zones' motion from the direction of temperature gradient.

### 4 Annular zones

It was experimentally established that the annular zones on silicon wafers  $\{100\}$  transform into square ones during migration in the direction  $\langle 100 \rangle$  (Fig. 4). By

**Fig. 4** Photos of wafer  $\{100\}$  with epitaxial channel. It illustrates sequential transformation of annular zone into the square one during the migration in direction  $\langle 110 \rangle$  on different distances from starting surface of wafer: 10  $\mu\text{m}$  (a); 80  $\mu\text{m}$  (b); 170  $\mu\text{m}$  (c); 480  $\mu\text{m}$  (d). The outer diameter of the ring (a) is 2.5 mm



metallographic analysis it was revealed that the transformation begins with the appearance of facet planes  $\{111\}$  at four symmetrically located points on the outer contour of the annular zone (marked with arrows in Fig. 4a). As the zone migrates into the wafer, straight sections of the zone appear at these points along the directions  $\langle 110 \rangle$ . The facets do not appear on the inner contour of the zone. The length of the straight sections of the zone increases monotonously during migration up to the formation of a linear zone in the form of a square (see Fig. 4d). As a result, a closed epitaxial channel forms in the silicon wafer. It has four wedge-shaped sides directed at a certain angle to the normal. The magnitude of this angle was weakly dependent on the temperature gradient and significantly on the temperature of the process. Thus, at temperatures of 1320, 1370, 1440 and 1570 K, the angle had values of 30, 25, 20 and 15° respectively. Therefore, at higher temperatures of thermomigration, a greater distance is required, traversed by the zone in the crystal for the transformation of the annular zone into a square one, or at a higher temperature closed channels are formed that differ less from the cylindrical shape.

It is established that the migration of the annular zone in the wafer  $\{111\}$  in the direction  $\langle 111 \rangle$  is accompanied by its' transformation into the form of an equilateral triangle, with the sides oriented along the directions  $\langle 110 \rangle$ . In this

case, the transformation of the zone began by faceting the outer contour of the zone with lateral planes  $\{111\}$  at three points equidistant from each other. The inner contour of the zone did not show facet. The evolution of the facet during migration led to the formation of three straight sections of the zone, the trajectories of which deviated from the normal by an angle of  $\sim 10^\circ$  at a process temperature of 1370 K.

## 5 Force model

To explain the observed instabilities of the motion of linear zones due to silicon anisotropy in the known force model [18], it is necessary to give a vector meaning to the forces of movement resistance in various sections of the zone dissolution front and consider them proportional to the area of the sections and perpendicular to them.

The anisotropic properties of silicon are emerged in faceting planes  $\{111\}$  only at the dissolution front. The absence of a facet of the crystallization front indicates the isotropy of this process during thermomigration of linear zones. Diffusion in the liquid zone is also isotropic. Therefore, the processes of crystallization and atomic transfer will not contribute to the deviation of the trajectory of the zone from the direction of the temperature gradient and



they can be neglected. Let's imagine the driving force of thermomigration in the form of three terms  $F = F_d + F_c + F_r$ , corresponding to three interrelated processes, characterized by coefficients of movement resistance  $R_d, R_c, R_r$  (see the formula for velocity given in the background).

In stationary migration conditions, the vector sum of the resistance forces in all sections of the dissolution front must be balanced with the driving force acting on the dissolution front  $-F_d$ . This makes possible to predict the direction of the linear zone migration in an anisotropic crystal. In the proposed model, there is no need to determine considered forces, it is enough to establish the relationship between them using a cross-section of the zone.

For example, we present estimation of the effect of silicon anisotropy on the trajectory of a rectilinear zone oriented in the direction  $\langle 110 \rangle$  with the temperature gradient in the direction  $\langle 111 \rangle$  (see Fig. 3). The forces on the dissolution front are shown in Fig. 3b. At these orientations, as already noted, the dissolution front has two planes of facet  $\{111\}$ : frontal and lateral, which correspond to the frontal  $F_f$  and lateral  $F_s$  resistance forces. The resistance forces at these sections arise as a reaction to the external thermal force  $F_d$ .

In the results of the analysis of the cross sections of wafers with linear zones, it was found that the area of the frontal face is much larger than the area of the lateral one. In particular, at a temperature of 1370 K and a temperature gradient of 60 K/cm, this ratio is 5.5. Then, the relationship between the resistance forces per unit length of the linear zone is determined by the equation:  $F_f = 5.5 F_s$ . In stationary conditions (velocity is constant), the thermal force  $F_d$  acting at the dissolution front, coinciding in the direction with the temperature gradient  $G$ , must be balanced by the resistance forces  $F_f$  and  $F_s$ . Balancing these forces vertically (see Fig. 3b) leads to the equation:  $F_d = 5.5 F_s + F_s \sin \beta$ . However, the horizontal component of  $F_s$  the modulus of which is  $F_s \cos \beta$ , remains uncompensated. It leads to a tangential component of the velocity of the movement of the zone and deviation of resulting velocity  $v_r$  from the temperature gradient  $G$  by an angle  $\gamma$  (Fig. 3b). Horizontal component of force  $F_s$  is compensated by counter resistance force, appearing at the right edge of dissolution front, the area of which increase due to decreasing area of zone's crystallization. Angle  $\gamma$  is defined by the expression:  $\tan \gamma = \cos \beta / (5.5 + \sin \beta)$ . The angle  $\beta$ , as can be seen from Fig. 3b, is  $20^\circ$ , then the angle  $\gamma \approx (9 \pm 1)^\circ$ . Thus, the reason for the deviation of the direction of movement of the linear zone from the temperature gradient is due to the asymmetric faceting of the dissolution front of the zone, which leads to the presence of a component of the resistance force directed along the surface of the silicon wafer.

## 6 Results and discussion

Let us apply the proposed force model to the annular zone migrating through a  $\{111\}$  silicon wafer. At the initial stage (at the start) of the movement of the annular zone, there are three sections on its outer contour, the tangents of which coincide with the  $\langle 110 \rangle$  directions where the lateral faces  $\{111\}$  are emerged at the dissolution front. The considered forces lead to the displacement of these rectilinear sections of the zone inside the circle during the migration of the entire zone normally to the wafer. The length of these sections increases until the outer contour of the annular zone takes the form of an equilateral triangle. The inner contour of the facet of the zone is absent. The sections of the annular zone that correspond to the vertices of this triangle migrate normally to the wafer without deviating from the temperature gradient. This follows from the fact that the equilateral triangle shape is inscribed in the outer contour of the annular zone at the start. The measured value of the deviation of straight section of annular zone from normal is  $\sim 10^\circ$ , which is consistent with theoretical estimation.

The transformation of the annular zone into a square zone during thermomigration in the direction  $\langle 100 \rangle$  is explained by the presence of four points on the annular zone, the tangents to which coincide with the directions  $\langle 110 \rangle$ , where the nucleations of the planes  $\{111\}$  occur on the outer contour of the zone (Fig. 4).

The substantiation for the faceting of the dissolution front and the absence of it at the crystallization front is due to the difference in the sign of these fronts' curvature. The advance of the faceted front occurs by a layered atomic kinetic mechanism and requires a source of atomic steps on a singular surface. The rectilinear zone has a convex dissolution front and a concave crystallization front. Therefore, there are always stairs that facilitating the growth of the crystal, and facet does not occur. The convex dissolution front of the zone with positive curvature excludes the presence of natural steps and is faceted in silicon by densely packed planes  $\{111\}$ . The dissolution of such planes occurs by dislocation or two-dimensional nucleation mechanism.

On the inner contour, the dissolution front of the annular zone with a negative curvature of the surface faceting does not occur due to the absence of planes  $\{111\}$  coherent to this front. As a result, a lateral force is occurred at these four points, directed into the annular zone. The length of the faceted rectilinear sections of the annular zone increases during the migration of the zone, and the annular zone turns into a square one. The observed decrease of deviation angle of the trajectory motion of the rectilinear sections of the zone from the temperature gradient indicates a weakening of the effect of the anisotropy of the silicon on the stability of the annular zone with an increase in the process temperature.

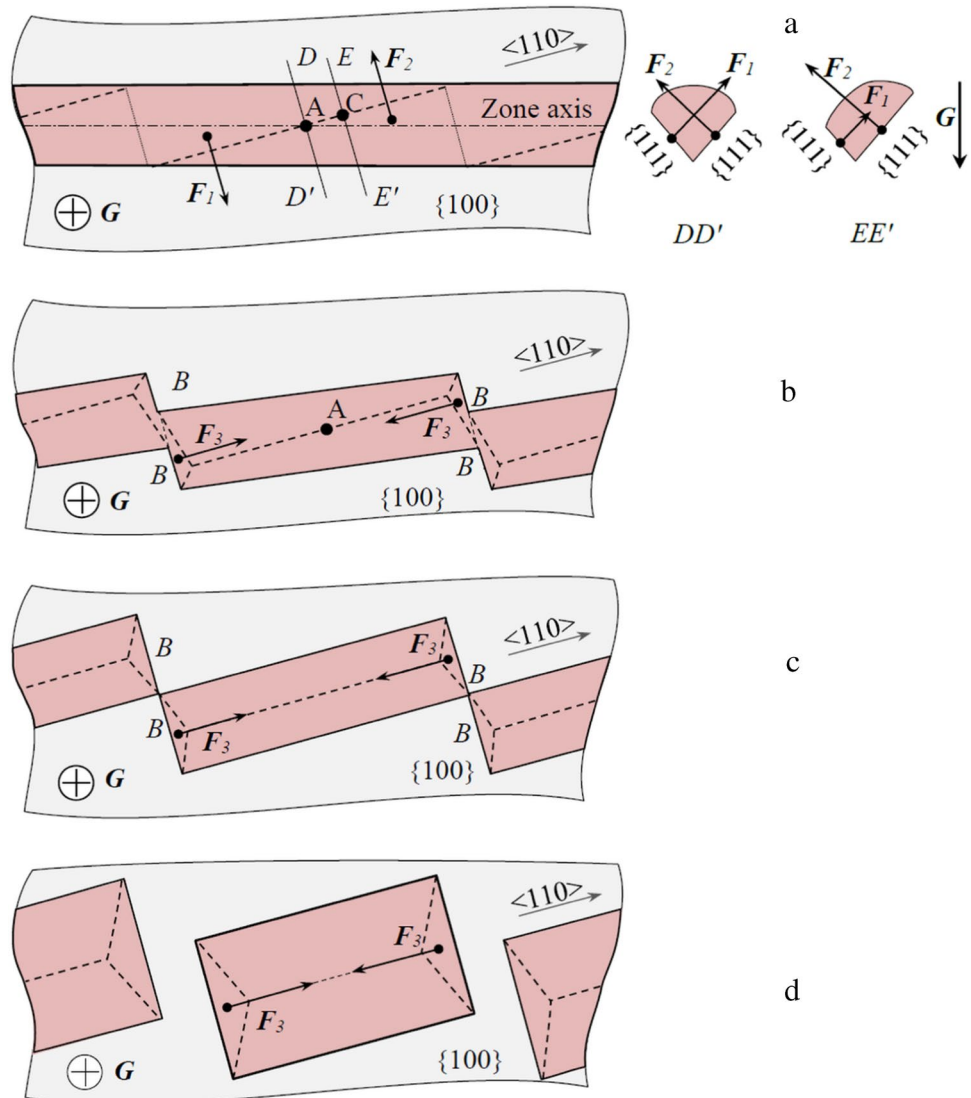
Proposed force model also explains the instabilities that arise at the ends of rectilinear zones (Fig. 2). The end of the rectilinear liquid zone inside the crystal has a rounded shape due to the surface tension forces. If the  $\langle 110 \rangle$  direction is tangent to the middle part of the rounded end of the zone (within  $\sim 20^\circ$  between the normal to the zone axis), then this leads to the appearance of a lateral face  $\{111\}$  at the dissolution front at the end of the zone. As a result, a force appears, which leads to the displacement of the liquid phase along the zone and the thickening of the end of the rectilinear zone. If the  $\langle 110 \rangle$  direction forms a tangent to the rounded end of the zone not in the middle part of the end of the zone at an angle more than  $\sim 20^\circ$  between the normal to the zone axis, then the lateral facet of the dissolution front leads to a force directed at an angle to the zone axis, which causes the observed kinks of rectilinear zones along the  $\langle 110 \rangle$  direction (Fig. 2).

The thickening of the end of the rectilinear zone, oriented in the  $\langle 110 \rangle$  direction and migrating in the  $\langle 100 \rangle$  direction, is associated with the presence of another plane  $\{111\}$  at the dissolution front in the end of the zone at an angle of  $125^\circ$  to the axis of the zone with respect to the normal to the surface of the wafer in addition to planes  $\{111\}$  shown in Fig. 1a.

Proposed model also explains the mechanism of fragmentation and decay of initially rectilinear zone migrating in the  $\langle 100 \rangle$  direction if the orientation of the zone does not coincide with the  $\langle 110 \rangle$  direction. In this case, the dissolution front is also faceted by two planes  $\{111\}$ , as for the oriented zone in the direction  $\langle 110 \rangle$ , but the line of intersection of these planes does not coincide with the axis of the zone (Fig. 5a).

The area of the faceting planes within the fragments of the zone varies, causing changes in the magnitude of the resistance forces to the movement of zone  $F_1$  and  $F_2$  along

**Fig. 5** Diagram of fragmentation and decay of a rectilinear zone migrating in the direction  $\langle 100 \rangle$  when the zone axis deviates from the  $\langle 110 \rangle$  direction. *a, b, c, d* – sequential stages of zone transformation (fragments at the initial stage of the process are separated from each other by a dotted line). In insertion (*a*) – cross-sections *DD'* and *EE'* of the zone



the line of intersection of the planes. The vector sums of forces  $F_1$  and  $F_2$  in each section normal to the line of intersection of the  $\{111\}$  planes have components along the surface  $\{100\}$ , except for the sections at the midpoint A of the zone fragment, where  $F_1 = F_2$  (Fig. 5a). For example, Fig. 5a shows the cross-sections  $DD'$  and  $EE'$  of the zone fragment and the acting forces of resistance. As a result, in each quadrangular fragment of the zone during thermomigration a torque occurs that rotates it around point A in the plane  $\{100\}$  of the wafer. The rotation of the fragment ends when its' boundaries coincide with the direction  $\langle 110 \rangle$  (Fig. 5c). The linear zone takes on a stair-like appearance with rectangular fragments. At the same time, new faceting  $\{111\}$  planes and resistance forces  $F_3$  emerge at the end faces B of the fragments, driving the movement of the liquid phase along the fragments and causing their separation from each another (Fig. 5b, c, d). As the migration continues, the fragments become shorter and thicker under the action of the end forces  $F_3$ , and the distances between them increase (Fig. 5d). Form of fragments in the plane  $\{100\}$  strive to rectangular during thermomigration. These results correspond our experimental observations and for the first time allows to explain the mechanism of fragmentation and decay of the zones [15, 16].

## 7 Conclusions

The patterns of thickenings and kinks formation of ends of rectilinear zones and the transformation of annular linear zones into triangular or square zones during their migration in silicon wafers  $\{111\}$  and  $\{100\}$  have been experimentally established. A force model of thermomigration is proposed to explain the transformation of annular linear zones, as well as the behavior of the ends and fragmentation of rectilinear zones. The model is based on the assumption that the resistance forces to movement caused by the planes  $\{111\}$  faceting the dissolution front of the zone are normal to these planes and proportional to their areas. Balancing these forces with the driving thermal force acting on the dissolution front of the zone makes it possible to determine the direction of migration of the linear zone in anisotropic silicon. To predict possible distortions of a specified shape of linear zones and formed epitaxial channels, it is necessary to identify the zones of the facet planes that are coherent to the dissolution front and estimate the vector sum of all the resistance forces to movement.

**Author contributions** B.M. Seredin — conceptualization, methodology, supervision, investigation, data analysis.

V.P. Popov — methodology, investigation, data acquisition and analysis.

A.M. Malibashev — methodology, investigation, data acquisition and analysis.

I.V. Gavrus — investigation, data acquisition and analysis.

S.M. Loganchuk — investigation, data acquisition and analysis.

S.Y. Martyushov — investigation, data acquisition and analysis.

All authors participated in the preparation and editing of the original draft.

**Funding** The study was supported by the Ministry of Science and Higher Education of the Russian Federation within the State assignments for Platov South-Russian State Polytechnic University (program FENN-2023–005).

**Data availability** The datasets generated during and/or analysed during the current study are available from the corresponding author on reasonable request.

## Declarations

**Competing interests** The authors declare no competing interests.

## References

1. Pfann WG (1963) Zone Melting, 2nd edn. Wiley and Sons, New York
2. Lozovskii VN, Lunin LS, Popov VP (1987) Zone recrystallization by temperature gradient. Metallurgy, Moscow
3. Lozovskii VN, Popov VP, Seredin BM (2015) Comparing diffusion and epitaxial methods for obtaining radiation-resistance structures of power semiconductor devices Questions of atomic science and technics. Series: Physics of radiation effects on radio-electronic equipment 3:57–61
4. Anthony TR, Boah JK, Chang MF, Cline HE (1976) Thermomigration processing of isolation grids in power structures. IEEE Trans Electron Devices 23(8):818–823. <https://doi.org/10.1109/T-ED.1976.18492>
5. Chang M, Kennedy R (1981) The application of temperature gradient zone melting to silicon wafer processing. J Electrochem Soc 10(1149/1):2127216
6. Lu B, Gautier G, Valente D, Morillon B, Alquier D (2016) Etching optimization of post aluminum-silicon thermomigration process residues. Microelectron Eng 149:97–105. <https://doi.org/10.1016/j.mee.2015.10.004>
7. Morillon B, Dilhac JM, Ganibal C, Anceau C (2003) Study of aluminum thermomigration as a low thermal budget technique for innovative power devices. Microelectron Reliab 43(4):565–569. [https://doi.org/10.1016/S0026-2714\(03\)00025-8](https://doi.org/10.1016/S0026-2714(03)00025-8)
8. Norskog AC, Warner RM (1981) A horizontal monolithic series-array solar battery employing thermomigration. J Appl Phys 52(3):1552–1554. <https://doi.org/10.1063/1.329637>
9. Lomov AA, Punegov VI, Seredin BM (2021) Laue X-ray diffraction studies of the structural perfection of Al-doped thermomigration channels in silicon. J of Appl Cryst 54:588–596. <https://doi.org/10.1107/S1600576721001473>
10. Lomov AA, Punegov VI, Belov AY, Seredin BM (2022) High-resolution X-ray Bragg diffraction in Al thermomigrated Si channels. J of Appl Cryst 55:558–568. <https://doi.org/10.1107/S1600576722004319>
11. Seidensticker RG (1966) Kinetic effects in temperature gradient zone melting. J Electrochem Soc 113(2):152–155. <https://doi.org/10.1149/1.2423890>

12. Mullins W, Sekerka RF (1963) Morphological stability of a particle growing by diffusion or heat flow. *J Appl Phys* 34(2):323–329. <https://doi.org/10.1063/1.1702607>
13. Lozovskii VN, Popov VP (1972) Stability of zone melting with gradient temperature. *Crystallography* 17(6):1232–1237
14. Lozovskii VN, Ovcharenko AN, Popov VP (1986) Liquid-solid interface stability. *Prog Crystal Growth Charact* 13(3):145–162
15. Lozovskii VN, Popov VP (1970) Stability of growth front in the method of moving solvent. *Crystallography* 15(1):149–155
16. Cline HE, Anthony TR (1976) High-speed droplet migration in silicon. *J Appl Phys* 47(6):2325–2331. <https://doi.org/10.1063/1.323008>
17. Cline HE, Anthony TR (1976) Thermomigration of aluminum-rich liquid wires through silicon. *J Appl Phys* 47(6):2332–2336. <https://doi.org/10.1063/1.323009>
18. Popov VP (1988) Non-conservative liquid phase epitaxy of semiconductors. *Sov Phys J* 31(1):51–56
19. Lozovskii VN, Popov VP, Malibasheva LY (1970) Trajectory of liquid inclusions in thermomigration in anisotropic crystal. *Crystallography* 20(1):991–994

**Publisher's Note** Springer Nature remains neutral with regard to jurisdictional claims in published maps and institutional affiliations.

Springer Nature or its licensor (e.g. a society or other partner) holds exclusive rights to this article under a publishing agreement with the author(s) or other rightsholder(s); author self-archiving of the accepted manuscript version of this article is solely governed by the terms of such publishing agreement and applicable law.